Original Article

Energy Window and Contrast Optimization for Single-photon Emission Computed Tomography Bremsstrahlung Imaging with Yttrium-90

Youssef Bouzekraoui, Farida Bentayeb, Hicham Asmi, Faustino Bonutti[1]

Department of Physics, LPHE, Modeling and Simulations, Faculty of Science, Mohammed V University, Rabat, Morocco, [1]Department of Medical Physics, Academic Hospital of Udine, Udine, Italy

Abstract

Purpose: In yttrium-90 (Y-90) single-photon emission computed tomography (SPECT) imaging, the choice of the acquisition energy window is not trivial, due to the continuous and broad energy distribution of the bremsstrahlung photons. In this work, we investigate the effects of the energy windows on the image contrast to noise ratio (CNR), in order to select the optimal energy window for Y-90 imaging. **Materials and Methods:** We used the Monte Carlo SIMIND code to simulate the Jaszczak phantom which consists of the six hot spheres filled with Y-90 and ranging from 9.5 to 31.8 mm in diameter. Siemens Symbia gamma camera fitted with a high-energy collimator was simulated. To evaluate the effect of the energy windows on the image contrast, five narrow and large energy windows were assessed. **Results:** The optimal energy window obtained for Y-90 bremsstrahlung SPECT imaging was 120–150 keV. Furthermore, the results obtained for CNR indicate that the high detection is only for the three large spheres. **Conclusion:** The optimization of energy window in Y-90 bremsstrahlung has the potential to improve the image quality.

Keywords: *Bremsstrahlung, CNR, Jaszczak phantom, SIMIND, yttrium-90 single-photon emission computed tomography imaging*

Introduction

In gamma camera imaging, the acquisition energy window is centered around photopeak to detect majority of primary photons. However, for yttrium-90 (Y-90) bremsstrahlung, as the acquired spectrum is complex and continuous, the choice of acquisition energy windows is one of the most challenging topics in nuclear medicine.[1] Several works have been performed in the objective to optimize bremsstrahlung imaging.[2-6] However, no study has evaluated the image quality and accurate activity quantification for Y-90 bremsstrahlung in terms of contrast and contrast to noise ratio and also geometric, penetration, and scatter components. In this study, a Monte Carlo simulation SIMIND code[7] was used to investigate the effects of the energy windows, using a high-energy (HE) collimator on the image contrast and signal to noise ratio (CNR), in order to optimize the Y-90 bremsstrahlung single-photon emission computed tomography (SPECT) imaging. The simulations were set up in such a way that it provides geometric, penetration, and scatter components to a separate file. At the end of simulations, binary images were imported in ImageJ software (Version 1.51) National Institutes of Health and the Laboratory for Optical and Computational Instrumentation (LOCI, University of Wisconsin).[8]

Materials and Methods

We simulated the Siemens Medical System Symbia equipped with a HE collimator and with detector having the following characteristics: 0.95 cm NaI (Tl) crystal thickness, 50 cm × 50 cm of area, intrinsic spatial resolution of 0.360 cm, and energy resolution of 10% at 140 keV. The collimator data used during the simulation are given in Table 1.

Bremsstrahlung energy spectra were generated with SIMIND Monte Carlo code (version 6.1) by simulating six spheres of different sizes filled with Y-90 and located inside water cylindrical phantom (L: 10 cm, rayon 1: 11 cm, and rayon 2: 12 cm). The inner diameters of the six spheres used are: 3.7, 2.8, 2.2, 1.7, 1.3, and 1 mm. The activity concentration for the six spheres was 3.374 MBq/mL. The

How to cite this article: Bouzekraoui Y, Bentayeb F, Asmi H, Bonutti F. Energy window and contrast optimization for single-photon emission computed tomography bremsstrahlung imaging with yttrium-90. Indian J Nucl Med 2019;34:125-8.

Address for correspondence:
Dr. Youssef Bouzekraoui, Laboratory of High Energy Physics and Monte Carlo Simulation, Faculty of Sciences, University Mohammed V, Rabat, Morocco.
E-mail: youssef0fsr@gmail.com

Access this article online

Website: www.ijnm.in

DOI: 10.4103/ijnm.IJNM_150_18

Quick Response Code:

Table 1: Collimator specifications

Collimator	Diameter (cm)	Septa (cm)	Length (cm)	Hole shape	Col type
HE	0.400	0.200	5.970	Hexagonal	Parallel hole

HE: High energy

phantom was positioned at 15 cm from the detector surface. The projections were generated in matrices of 256 × 256 pixels, 0.24 cm pixel size, 128 views, and 360° clockwise gantry rotation. The simulation is done, starting with large acquisition windows [Table 2]. In order to refine the results, narrower acquisition windows were considered [Table 3].

Contrast and CNR were calculated by the following formulas:

$$\text{Contrast } = \frac{C_s}{C_b} - 1$$

$$\text{CNR} = (C_s - C_b) \times \frac{Voxel}{\sqrt{\sigma_s^2 + \sigma_b^2}}$$

$C_S = S_C/V_S$: Number of counts in the spheres per voxel

SC: Total counts in the spheres
VS: Sphere volume in number of voxels
$C_b = N_C/V_B$: Number of counts in the background compartment per voxel
N_C: Total counts in the background compartment
V_B: Background volume in number of voxels
σ_s:The variance in sphere

σ_b: The variance in background.

Results

Figure 1 shows the energy spectrum as a function of energy for Y-90.

As shown in Figure 2, the geometric component rehearses a high value in 135 keV for 1st acquisition and 130 keV in the second. Whereas, the scatter and penetration components are small at this energy in both cases.

Figure 3 shows the effects of the energy window on the image contrast of the hot spheres with HE collimator. In comparison, both energy windows centered at 135 keV for 1st and 2nd acquisition provide a higher contrast than the others.

Figures 4 and 5 show the effect of energy windows on the image quality of the simulated Jaszczak phantom with six hot spheres.

We notice, as shown in Figure 6, that when the energy increases, the CNR decreases, and therefore, the image quality decreases. We observed the best CNR values for the first two energy windows in both acquisitions. In these windows, we can distinguish the two large spheres very well, but it is hard to distinguish the three smallest spheres. This seems to have been caused by increased background noise due to large penetration.

Table 2: Size and central position for the sub-windows of the large window-set

	1	2	3	4	5
Subwindow (keV)	30–100	100–170	170–240	240–310	210–380
Center (keV)	65	135	205	275	345

Table 3: Size and central position for the sub-windows of the narrow window-set

	1	2	3	4	5
Subwindow (keV)	60–90	90–120	120–150	150–180	180–210
Center (keV)	75	105	135	165	195

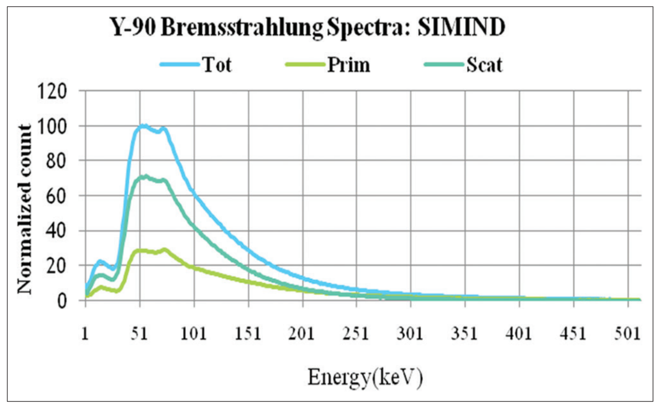

Figure 1: Monte Carlo simulated spectrum for yttrium-90

Discussion

In Y-90 bremsstrahlung imaging, the image quality and quantification are limited due to the high levels of object scatter, collimator septal penetration, and collimator scatter. The parallel hole collimator and energy window optimization in Y-90 have been studied.[1-6] In this study, we used Monte Carlo simulation SIMIND code to demonstrate how the image quality degrades as function of imaging parameters. We have evaluated the image quality considering the contrast and contrast to noise ratio (CNR). The simulation data indicates that the choice of the acquisition energy window for Y-90 imaging has a great effect on the image contrast and contrast to noise ratio. Figure 3 shows the high contrast values in 135 keV center for both acquisitions. We notice, as shown in Figure 6, that the best CNR values are obtained in the first three windows. The simulations also show that the penetration is a significant problem for HE collimator at HE. The HE collimator with an energy window between 120 and 150 keV was selected as optimal acquisition setting with consideration of the contrast and contrast to noise ratio (CNR) and also geometric, penetration, and scatter

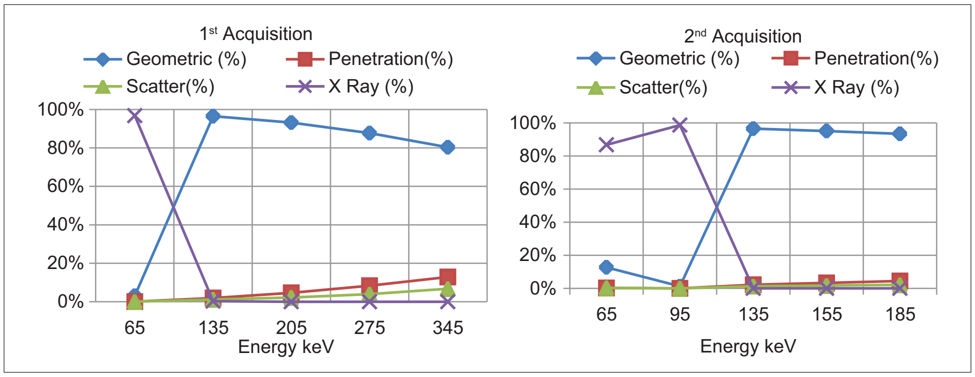

Figure 2: Contributions of geometric, penetration, scatter, and X-rays components with energy windows

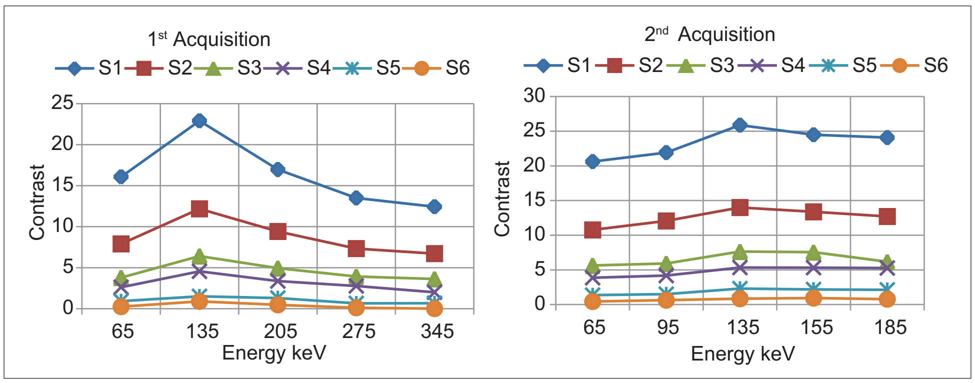

Figure 3: Contrast of the six spheres with energy window

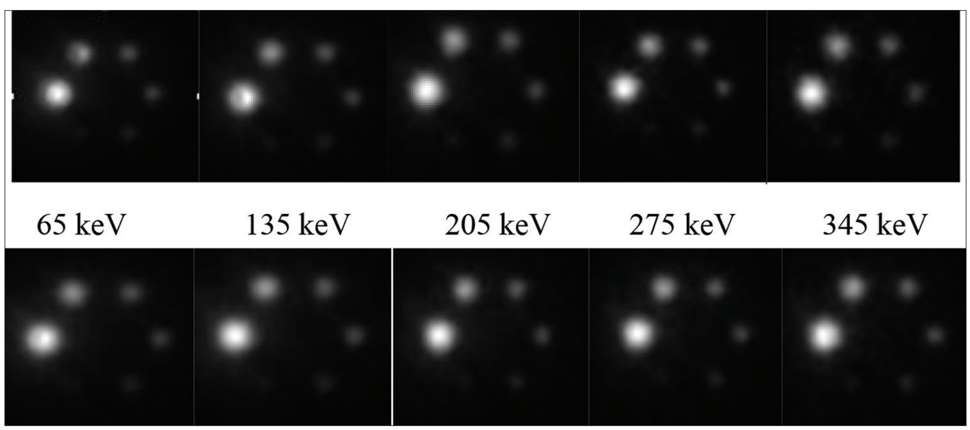

Figure 4: Images of simulated Jaszczak phantom with a high-energy collimator using large energy windows (above) and narrow energy windows (below)

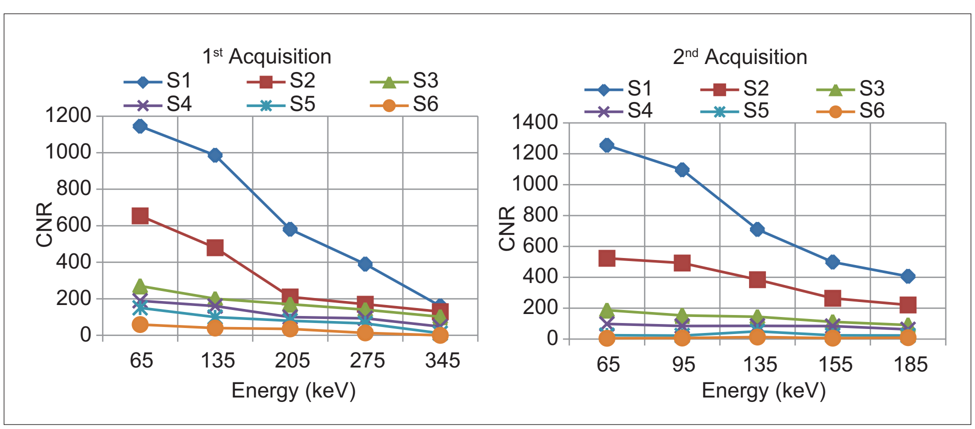

Figure 5: CNR of the six spheres

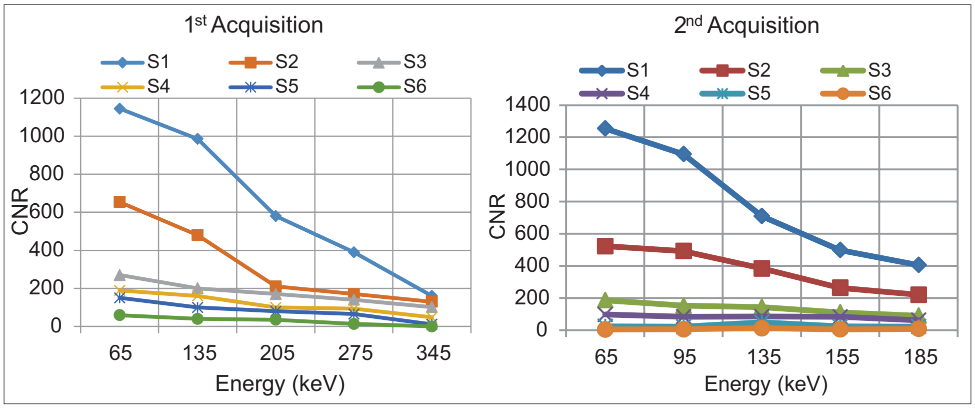

Figurer 6: CNR of the six spheres with energy windows

photons. The optimization of collimator and acquisition energy window leads to improve the quantitative accuracy and Y-90 bremsstrahlung SPECT image quality.

Conclusion

In this study, the obtained results showed that the HE parallel-hole collimator with energy window 120–150 keV conditions provides the best imaging performance based on contrast and CNR values. The optimization of these parameters leads to improved treatment efficacy and Y-90 bremsstrahlung SPECT imaging.

Financial support and sponsorship

Nil.

Conflicts of interest

There are no conflicts of interest.

References

1. Rong X, Du Y, Ljungberg M, Rault E, Vandenberghe S, Frey EC, *et al.* Development and evaluation of an improved quantitative (90) Y bremsstrahlung SPECT method. Med Phys 2012;39:2346-58.
2. Heard S, Flux GD, Guy MJ, Ott RJ. Monte Carlo simulation of 90Y bremsstrahlung imaging. IEEE Nucl Sci Symp 2004;7:3579-83.
3. Roshan HR, Mahmoudian B, Gharepapagh E, Azarm A, Pirayesh Islamian J. Collimator and energy window optimization for 90Y bremsstrahlung SPECT imaging: A SIMIND Monte Carlo study. Appl Radiat Isot 2016;108:124-8.
4. Rong X, Frey EC. A collimator optimization method for quantitative imaging: Application to Y-90 bremsstrahlung SPECT. Med Phys 2013;40:082504.
5. Rong X, Ghaly M, Frey EC. Optimization of energy window for 90Y bremsstrahlung SPECT imaging for detection tasks using the ideal observer with model-mismatch. Med Phys 2013;40:062502.
6. Rong X, Du Y, Frey EC. A method for energy window optimization for quantitative tasks that includes the effects of model-mismatch on bias: Application to Y-90 bremsstrahlung SPECT imaging. Phys Med Biol 2012;57:3711-25.
7. Ljungberg M. The SIMIND Monte Carlo Program Home Page. Available from: https://www.msf.lu.se/forskning/the-simind-monte-carlo-program. [Last accessed on 2018 Oct].
8. Ferreira T, Rasband W. Image J Program. Available from: https://www.imagej.nih.gov/ij/download.html. [Last accessed on 2018 Oct].